Imaging Probes

DOI: 10.1002/ange.200903556

Imparting Multivalency to a Bifunctional Chelator: A Scaffold Design for Targeted PET Imaging Probes**

*Wei Liu, Guiyang Hao, Michael A. Long, Tiffani Anthony, Jer-Tsong Hsieh, and Xiankai Sun**

Positron emission tomography (PET) has become a standard clinical practice in the diagnostic or prognostic imaging of cancer, mainly owing to the great success of [^{18}F]FDG (2-deoxy-2-^{18}F-fluoro-D-glucose) for non-invasive detection of glucose uptake in tumors.[1] Currently ^{11}C and ^{18}F are the most commonly used PET nuclides for the development of PET imaging probes. However, the short half-lives of these two radioisotopes (^{11}C $t_{1/2} = 20.3$ m, ^{18}F $t_{1/2} = 109$ m) limit their applications to biomolecules with relatively fast in vivo biodistribution kinetics, and the chemical procedures to incorporate these isotopes must be carried out in the proximity of a biomedical cyclotron. Among nonstandard PET nuclides, ^{64}Cu ($t_{1/2} = 12.7$ h; β^+ 0.653 MeV, 17.4%) has drawn considerable interest in PET research owing to its low positron range, commercial availability, and reasonably long decay half-life. Such characteristics could enable a variety of imaging applications involving peptides, antibodies or their fragments, and nanoparticles.[2,3]

It has been demonstrated that creation of multimers of a targeting molecule on one scaffold can efficiently improve cell-specific binding affinity by several orders of magnitude.[3] As such, various approaches have been reported to exploit multivalent scaffolds for the construction of molecular imaging probes.[4–10] However, their chemistries are often complicated and become even more so when a bifunctional chelator (BFC) must be attached to a separately multimerized construct in order to introduce a metal radionuclide for nuclear imaging.

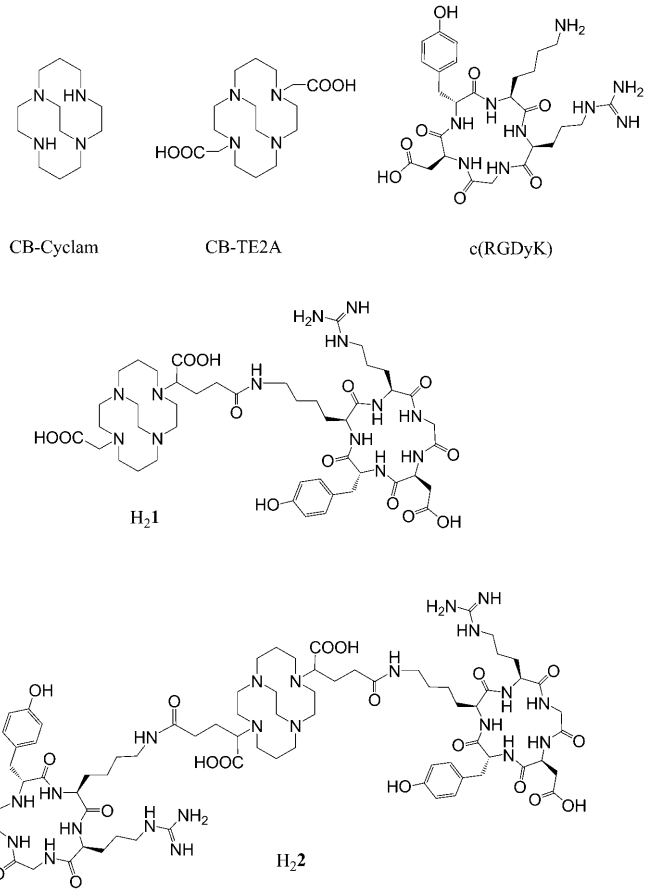

Scheme 1. Chemical structures of relevant compounds

Herein we present an approach to take advantage of the pendent arms of the commonly used BFCs to build simplified but potentially versatile multivalent scaffolds for multimeric presentation of targeting molecules. This type of multivalent scaffold features a chelator that forms a stable and neutral complex with a radiometal and multiple functional groups for the anchoring of targeting molecules. If required by in vivo pharmacokinetics, poly(ethylene glycol) (PEG) chains can be introduced between the chelate and targeting moieties.

To test the rationale of our design, we use a cyclic RGD peptide (c(RGDyK),[5,11] a well-validated $\alpha_v\beta_3$ integrin ligand, for the construction of a divalent PET imaging probe from a chelate known to have a high affinity for ^{64}Cu (CB-TE2A, Scheme 1). The divalent probe is anticipated to have a prolonged biological half-life and enhanced specific binding and retention in tissues expressing the $\alpha_v\beta_3$ integrin.

[*] W. Liu, G. Hao, M. A. Long, T. Anthony, X. Sun
Department of Radiology and Advanced Imaging Research Center
University of Texas Southwestern Medical Center
Dallas, TX 75390-8542 (USA)
Fax: (+1) 214-645-2885
E-mail: xiankai.sun@utsouthwestern.edu
J.-T. Hsieh
Department of Urology
University of Texas Southwestern Medical Center
Dallas, TX 75390-9110 (USA)

[**] This work was partially supported by a USAMRMC grant (W81XWH-08-1-0305) and two NIH grants (P01 DK058398; U24 CA126608). The authors acknowledge the generous support of a private donor that allowed the purchase of the Inveon PET-CT system. The c(RGDyK) peptide was provided by Dr. Xiaoyuan Chen at Stanford University

Supporting information for this article is available on the WWW under http://dx.doi.org/10.1002/anie.200903556.

The stability of the metal complex is of critical importance in the design of a metal radiopharmaceutical. CB-TE2A forms one of the most stable complexes with ^{64}Cu,[12] and the Cu^{II}-CB-TE2A complex is more resistant to reductive metal loss than are other tetramacrocyclic complexes.[13] However, its stability with ^{64}Cu may be reduced when used as a BFC in which one of the carboxylate groups is converted to an amide for conjugation to a targeting molecule,[14] leading to a positive charge on the ^{64}Cu moiety. To avoid this potential problem, we choose α-bromoglutaric acid-1-*tert*-butyl ester-5-benzyl ester (**3**) for the alkylation of CB-cyclam, which allows selective deprotection of the carboxylate groups by two separate procedures to conjugate with c(RGDyK) through the peripheral carboxylates to afford H_2**1** and H_2**2**, respectively. As such, the unique feature of CB-TE2A is preserved in the conjugates, in which the two inner carboxylates can form a neutral octahedral complex with $^{64}Cu^{II}$ along with the four nitrogen atoms of the macrocycle.

To evaluate the anticipated multivalent effect, a recently reported CB-TE2A analogue[15] was also synthesized and coupled with c(RGDyK) to form a monovalent CB-TE2A-RGD conjugate (H_2**1**) as a control for comparison. Scheme 2 shows the synthetic routes to H_2**1** and H_2**2**. The multiple-step synthetic route involves three parts: 1) synthesis of orthogonally protected compounds **5** and **7;** 2) formation of NHS-activated ester intermediates **6** and **9** after selective deprotection of the peripheral carboxylate groups (NHS = *N*-hydroxysuccinimide); and 3) conjugation of c(RGDyK) to the NHS esters followed by acid deprotection of the inner carboxylate groups to form the products H_2**1** and H_2**2**. Alkylation of CB-cyclam by **3** was asynchronous at the two nonbridged nitrogen atoms, with the monoalkylation product **4** predominating at room temperature (35–55% yield even in the presence of excess of **3**).[15] In comparison, the dialkylated product **7** was only formed at elevated temperatures. At 50 °C using two equivalents of **3** to CB-cyclam, only 20–45% of **7** was found, and it was always accompanied by the monoalkylation product. Although **7** was difficult to elute from silica gel using common organic solvents, a good separation was obtained by adding 5–10% isopropyl amine in ethyl acetate. It is noteworthy that the debenzylation of the peripheral carboxylate groups catalyzed by 10% Pd/C in a hydrogen atmosphere always resulted in formation of the corresponding esters if the reaction was carried out in an alcohol solvent. This finding is likely due to the "proton sponge" nature of the CB-cyclam core that induces transesterification during debenzylation. No clean debenzylization could be accomplished in either methanol or ethanol, even in the presence of formic acid as described in literature.[15] However, THF/H_2O (1:1) successful circumvented this problem and afforded debenzylation products in quantitative yield. These were then activated by NHS and conjugated to c(RGDyK) in the presence of ten equivalents *N*,*N*-diisopropylethylamine (DIPEA). After HPLC purification, H_2**1** and H_2**2** were obtained by removal of the *tert*-butyl groups using 95% trifluoroacetic acid (TFA; see the Supporting Information for details).

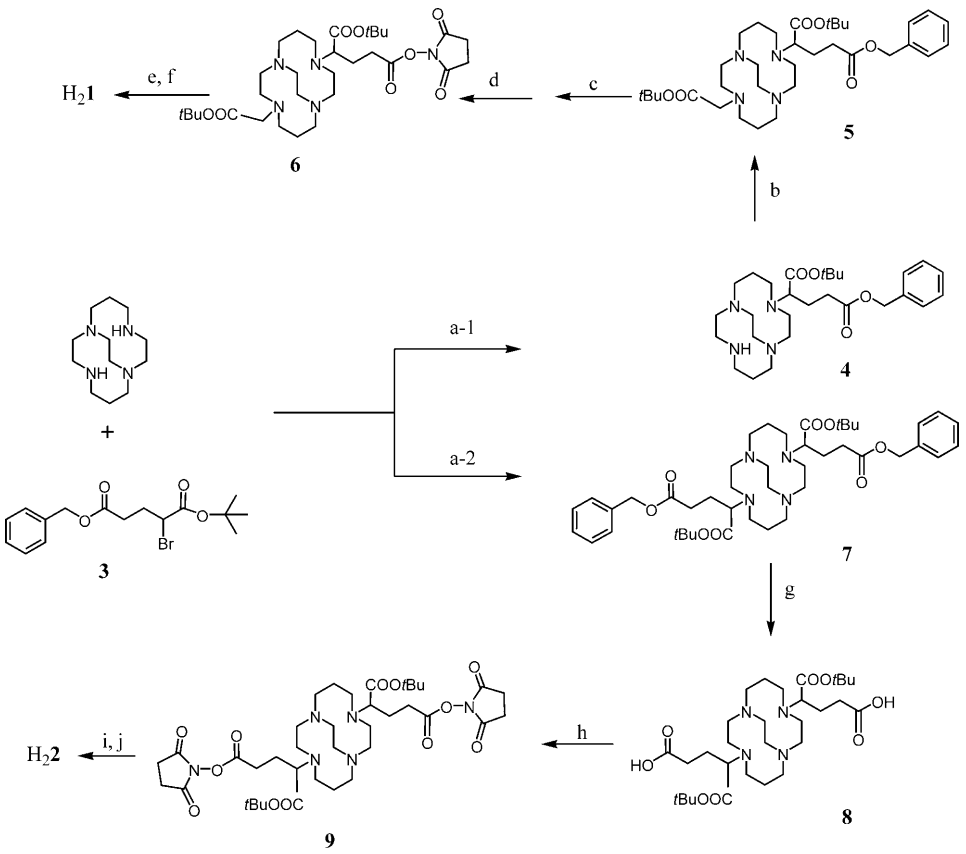

Scheme 2. Synthesis of H_2**1** and H_2**2**. Reagents: a-1, a-2) CH_3CN, K_2CO_3; b) $BrCH_2COOtBu$, CH_3CN, K_2CO_3; c, g) 10% Pd/C, THF/H_2O; d, h) MeCN, NHS, 1-ethyl-3-(3-dimethylaminopropyl)carbodiimide (EDC); f, i) c(RGDyK), DIPEA, DMF; e, j) 95% TFA.

Both H_2**1** and H_2**2** were efficiently labeled by ^{64}Cu at 70 °C in 0.4 M NH_4OAc buffer within 30 min. The specific activity of [^{64}Cu]**1** and [^{64}Cu]**2** was in the range of 8.4–20.4 GBq μmol^{-1}. The in vitro stability of the ^{64}Cu-labeled peptide conjugates was evaluated in rat serum by radio-HPLC. Chromatographic results showed no release of ^{64}Cu from the conjugates over a period of 48 h. This high stability is attributed to the CB-TE2A moiety in the conjugates. The $\alpha_v\beta_3$ binding affinities of H_2**1** and H_2**2** were measured by a competitive cell-binding assay using U87MG cells in which ^{125}I-echistation was employed as $\alpha_v\beta_3$-specific radioligand for

competitive displacement.[5] The U87MG cell line was chosen because the $\alpha_v\beta_3$ integrin density on the cell surface was the highest among the solid tumor cell lines that have been assessed.[16] The IC_{50} values of c(RGDyK), H_2**1**, and H_2**2**, which represent their concentrations required to displace 50% of the ^{125}I-echistation bound on the U87MG cells, were determined to be 110, 139, and 35 nM, respectively ($n=5$). The slightly decreased $\alpha_v\beta_3$ binding of H_2**1** as compared to c(RGDyK) indicates a minute impact of CB-TE2A on the binding of c(RGDyK) to the $\alpha_v\beta_3$ integrin. As anticipated, H_2**2** exhibited a strong divalent effect measured by the multivalent enhancement ratio (MVE) calculated by dividing the IC_{50} value of H_2**1** by that of H_2**2** (MVE = 4).[6] The distance between the two RGD motifs in H_2**2** is greater than 25 bonds (including the lysine spacers), the minimum spacing length required to realize multivalent binding of RGD motifs to the $\alpha_v\beta_3$ integrin.[5] It is noteworthy that as a downstream effect of multivalent binding, oligomerization of cell-surface receptors could initiate cellular internalization events, which might further enhance the specific accumulation in the target tissues.[17]

In vivo small-animal imaging studies were performed on a Siemens Inveon PET-CT multimodality system. Six SCID mice (6–7 weeks old) bearing PC-3 human prostate cancer xenografts in both front flanks (tumor size ca. 230 mg) were randomized into two groups ($n=3$) for the evaluation of [^{64}Cu]**1** or [^{64}Cu]**2**, which was injected into the tail vein. As shown in Figure 1, both tumors were visualized by [^{64}Cu]**1** and [^{64}Cu]**2** at 1 and 4 h post injection (p.i.), while [^{64}Cu]**2** showed a significantly stronger PET signal than [^{64}Cu]**1** at all time points. At 24 h p.i., the tumors were still clearly visible with [^{64}Cu]**2** but were rather faint with [^{64}Cu]**1**. Owing to the fact that the $\alpha_v\beta_3$ integrin is also expressed in other tissues (e.g. liver, kidneys, stomach, intestines) in young mice, but to a lesser extent (personal communications[18]), an elevated uptake was observed in those organs with [^{64}Cu]**2** as compared to [^{64}Cu]**1**. The enhanced tumor uptake and retention of [^{64}Cu]**2** may be partially attributed to the difference of in vivo kinetics of [^{64}Cu]**1** and [^{64}Cu]**2**, given the higher molecular weight of [^{64}Cu]**2**. Indeed, [^{64}Cu]**2** was not cleared as efficiently as [^{64}Cu]**1** from kidneys ([^{64}Cu]**1** 94.7 ± 3.6 %ID excreted at 24 h p.i.; [^{64}Cu]**2** 88.2 ± 4.9 %ID excreted at 24 h p.i.; $p < 0.05$). The $\alpha_v\beta_3$ binding specificity of [^{64}Cu]**1** and [^{64}Cu]**2** was demonstrated by signal loss (Figure 1: 1 h blockade) in tumors after co-injection of c(RGDyK) at a dose of 10 mg kg^{-1}. The quantitative PET image data and post-PET biodistribution data are presented in Table 1 and Tables S1–S3 (see the Supporting Information for details).

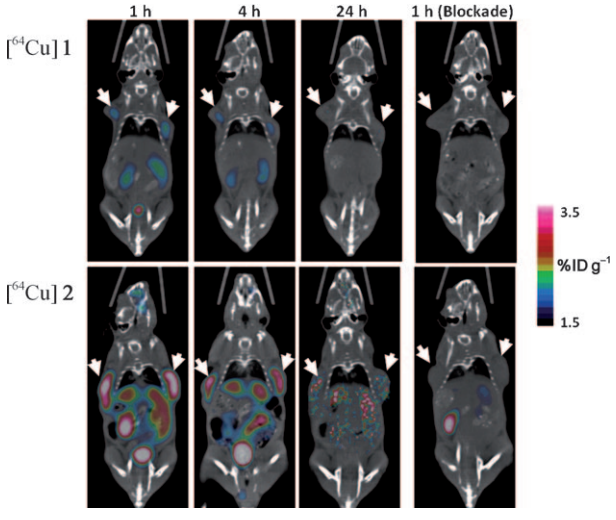

Figure 1. Representative microPET-CT images of PC-3 tumor bearing mice ($n=3$) at 1, 4, 24 h after intravenous injection of [^{64}Cu]**1** (upper panel) and [^{64}Cu]**2** (lower panel). Images obtained with co-injection of 10 mg kg^{-1} of c(RGDyK) are only shown for 1 h blockade (right). Arrows indicate tumors.

Table 1: Tumor uptake of [^{64}Cu]**1** and [^{64}Cu]**2** as determined from PET imaging quantitation and post-PET biodistribution. Data are presented as %ID g^{-1} ± standard deviation ($n=3$).[a]

	1 h PET	4 h PET	24 h PET	24 h Post-PET	1 h PET (blockade)
[^{64}Cu]**1**	1.95 ± 0.10	1.85 ± 0.26	1.10 ± 0.15	1.39 ± 0.17	0.31 ± 0.05
[^{64}Cu]**2**	2.92 ± 0.26	2.40 ± 0.22	1.72 ± 0.18	1.79 ± 0.13	0.71 ± 0.04

[a] For [^{64}Cu]**2**, $p < 0.05$ for all times.

The significantly greater uptake and prolonged signal intensity of [^{64}Cu]**2** in tumors reflects the advantages of the scaffolding design of H_2**2**, which affords optimal in vivo kinetics in addition to the anticipated multivalent effects. It should be pointed out that there are two chiral centers in the pendent arms of Cu**2**, which should statistically give rise to three diastereomers (*R*/*R*, *S*/*S*, and a meso *R*/*S*), even though they could not be distinguished by the techniques used herein. While the purpose of this work is to demonstrate the feasibility of building multivalent imaging probes from a bifunctional chelator, an enantiopure isomer of **3** should be considered for future clinical applications of this type of multivalent scaffold. Used as a sample targeting molecule herein, c(RGDyK) can obviously be replaced with other targeting peptides or small organic molecules for imaging of various diseases or non-invasive cell-surface receptor mapping. In summary, we have demonstrated a divalent scaffolding design for targeted imaging probe development. Obviously this concept can be applied to the design of other multivalent scaffolds based on NOTA (1,4,7-triazacyclononane-1,4,7-triacetic acid) or DOTA (1,4,7,10-tetraazacyclododecane-1,4,7,10-tetraacetic acid).

Received: June 30, 2009
Revised: July 18, 2009
Published online: September 1, 2009

Keywords: chelates · imaging agents · multivalent effect · radiochemistry

[1] M. Allen-Auerbach, W. A. Weber, *Oncologist* **2009**, *14*, 369.
[2] R. Rossin, S. Muro, M. J. Welch, V. R. Muzykantov, D. P. Schuster, *J. Nucl. Med.* **2008**, *49*, 103.
[3] R. Haubner, H. J. Wester, *Curr. Pharm. Des.* **2004**, *10*, 1439.

[4] A. Almutairi, R. Rossin, M. Shokeen, A. Hagooly, A. Ananth, B. Capoccia, S. Guillaudeu, D. Abendschein, C. J. Anderson, M. J. Welch, J. M. Frechet, *Proc. Natl. Acad. Sci. USA* **2009**, *106*, 685.
[5] Z. B. Li, W. Cai, Q. Cao, K. Chen, Z. Wu, L. He, X. Chen, *J. Nucl. Med.* **2007**, *48*, 1162.
[6] X. Montet, M. Funovics, K. Montet-Abou, R. Weissleder, L. Josephson, *J. Med. Chem.* **2006**, *49*, 6087.
[7] I. Dijkgraaf, J. A. Kruijtzer, S. Liu, A. C. Soede, W. J. Oyen, F. H. Corstens, R. M. Liskamp, O. C. Boerman, *Eur. J. Nucl. Med. Mol. Imaging* **2007**, *34*, 267.
[8] I. Dijkgraaf, A. Y. Rijnders, A. Soede, A. C. Dechesne, G. W. van Esse, A. J. Brouwer, F. H. Corstens, O. C. Boerman, D. T. Rijkers, R. M. Liskamp, *Org. Biomol. Chem.* **2007**, *5*, 935.
[9] M. Janssen, W. J. Oyen, L. F. Massuger, C. Frielink, I. Dijkgraaf, D. S. Edwards, M. Radjopadhye, F. H. Corstens, O. C. Boerman, *Cancer Biother. Radiopharm.* **2002**, *17*, 641.
[10] S. Liu, *Mol. Pharm.* **2006**, *3*, 472.
[11] W. Cai, S. S. Gambhir, X. Chen, *Methods Enzymol.* **2008**, *445*, 141.
[12] X. Sun, M. Wuest, G. R. Weisman, E. H. Wong, D. P. Reed, C. A. Boswell, R. Motekaitis, A. E. Martell, M. J. Welch, C. J. Anderson, *J. Med. Chem.* **2002**, *45*, 469.
[13] K. S. Woodin, K. J. Heroux, C. A. Boswell, E. H. Wong, G. R. Weisman, W. Niu, S. A. Tomellini, C. J. Anderson, L. N. Zakharov, A. L. Rheingold, *Eur. J. Inorg. Chem.* **2005**, 4829.
[14] M. Woods, P. Caravan, C. F. Geraldes, M. T. Greenfield, G. E. Kiefer, M. Lin, K. McMillan, M. I. Prata, A. C. Santos, X. Sun, J. Wang, S. Zhang, P. Zhao, A. D. Sherry, *Invest. Radiol.* **2008**, *43*, 861.
[15] C. A. Boswell, C. A. Regino, K. E. Baidoo, K. J. Wong, A. Bumb, H. Xu, D. E. Milenic, J. A. Kelley, C. C. Lai, M. W. Brechbiel, *Bioconjugate Chem.* **2008**, *19*, 1476.
[16] X. Zhang, Z. Xiong, Y. Wu, W. Cai, J. R. Tseng, S. S. Gambhir, X. Chen, *J. Nucl. Med.* **2006**, *47*, 113.
[17] J. E. Gestwicki, C. W. Cairo, L. E. Strong, K. A. Oetjen, L. L. Kiessling, *J. Am. Chem. Soc.* **2002**, *124*, 14922.
[18] S. Liu, unpublished results.

